Latent KSHV infection increases the vascular permeability of human endothelial cells

*Christophe Guilluy,[1] *Zhigang Zhang,[2,3] Prasanna M. Bhende,[2,3] Lisa Sharek,[1,2] Ling Wang,[2,3] Keith Burridge,[1,2,4] and Blossom Damania[2,3]

[1]Department of Cell and Developmental Biology, [2]Lineberger Comprehensive Cancer Center, [3]Department of Microbiology & Immunology, and [4]McAllister Heart Institute, University of North Carolina at Chapel Hill, Chapel Hill, NC

Kaposi sarcoma–associated herpesvirus (KSHV) is associated with 3 different human malignancies: Kaposi sarcoma (KS), primary effusion lymphoma, and multicentric Castleman disease. The KS lesion is driven by KSHV-infected endothelial cells and is highly dependent on autocrine and paracrine factors for survival and growth. We report that latent KSHV infection increases the vascular permeability of endothelial cells. Endothelial cells with latent KSHV infection display increased Rac1 activation and activation of its downstream modulator, p21-activated kinase 1 (PAK1). The KSHV-infected cells also exhibit increases in tyrosine phosphorylation of vascular endothelial (VE)–cadherin and β-catenin, whereas total levels of these proteins remained unchanged, suggesting that latent infection disrupted endothelial cell junctions. Consistent with these findings, we found that KSHV-infected endothelial cells displayed increased permeability compared with uninfected endothelial cells. Knockdown of Rac1 and inhibition of reactive oxygen species (ROS) resulted in decreased permeability in the KSHV-infected endothelial cells. We further demonstrate that the KSHV K1 protein can activate Rac1. Rac1 was also highly activated in KSHV-infected endothelial cells and KS tumors. In conclusion, KSHV latent infection increases Rac1 and PAK1 activity in endothelial cells, resulting in the phosphorylation of VE-cadherin and β-catenin and leading to the disassembly of cell junctions and to increased vascular permeability of the infected endothelial cells. (*Blood*. 2011;118(19):5344-5354)

Introduction

The endothelial cell barrier function is regulated by vascular endothelial (VE)–cadherin-containing adherens junctions in addition to tight junctions.[1] VE-cadherin is involved in maintaining the integrity of endothelial cell junctions by preventing the disassembly of the endothelial barrier and regulating the movement of macromolecules through the endothelium.[1-3] However, upon VEGF stimulation, these normal endothelial cell junctions are reorganized to allow the extravasation of cellular factors.[4] This involves the disruption of VE-cadherin at the adherens junction[2,4,5] and internalization of VE-cadherin from the cell surface.[6] VEGF stimulation leads to the induction of Rac1 activity[7,8] and its downstream effector, p21-activated kinase 1 (PAK1).[8] In addition, Rac1 has also been shown to regulate VE-cadherin phosphorylation through the generation of reactive oxygen species (ROS).[9,10]

Kaposi sarcoma (KS) is a multifocal vascular tumor of mixed cellular composition. KS lesions are composed of a mixed population of cells, including spindle-shaped endothelial cells and infiltrating leukocytes.[11,12] KS is the most common neoplasm in patients with AIDS. Areas that have the highest HIV burden, such as sub-Saharan Africa, also have the highest rate of KS. KS-associated herpesvirus (KSHV) is the etiological agent found in all epidemiologic forms of KS,[13] and viral genomic DNA is present in AIDS-associated KS, as well as in HIV-negative classic and transplantation-associated KS.[13,14] Since the discovery of the virus in KS, KSHV has also been consistently identified in primary effusion lymphoma and some forms of multicentric Castleman disease.[15-17] KSHV infection of the endothelial cells in the KS lesions is thought to drive proliferation of the tumor.

Three histological features of KS lesions are cellular proliferation, inflammation, and angiogenesis, and several studies have shown a high level of cytokines and chemokines within KS lesions.[18-21] The KS lesion has been shown to express high levels of VEGF and fibroblast growth factor, which are necessary for the maintenance of the angiogenic lesion.[19,22] In addition, KS-derived cells constitutively release matrix metalloproteinase 9 (MMP-9).[23] KSHV encodes for many proteins, and some of these are involved in cell proliferation and the up-regulation of angiogenesis. The viral G protein-coupled receptor (vGPCR) is a homolog of the human IL-8 receptor that induces expression of mitogenic and angiogenic growth factors including VEGF.[24,25] vIL6, a homolog of human IL-6, has also been implicated in the development of tumorigenesis and angiogenesis.[19] Our previous studies have shown that the KSHV K1 protein induces the secretion of VEGF, MMP-9, and also enhances angiogenesis and tumor size in vivo.[26,27] All 3 genes are expressed during the viral lytic cycle, but vIL6 and K1 are also expressed at low levels during viral latency.[26,28]

We have demonstrated previously that latent KSHV infection of endothelial cells induces the activation of the prosurvival PI3K/Akt/mTOR pathway.[29] Latent KSHV infection of endothelial cells

Submitted March 7, 2011; accepted July 27, 2011. Prepublished online as *Blood* First Edition paper, August 31, 2011; DOI 10.1182/blood-2011-03-341552.

*C.G. and Z.Z. contributed equally to this work.

The online version of this article contains a data supplement.

The publication costs of this article were defrayed in part by page charge payment. Therefore, and solely to indicate this fact, this article is hereby marked "advertisement" in accordance with 18 USC section 1734.

augments cell survival and increases the angiogenic potential of endothelial cells, even under conditions of stress.[29] Our present findings confirmed that latent KSHV infection of endothelial cells activates key pathways involved in promoting cell survival and angiogenesis, thereby contributing to the pathogenesis induced by KSHV in endothelial cells.

We report herein that latent KSHV infection of endothelial cells increases vascular permeability, and demonstrate that latent KSHV-infected endothelial cells display increased Rac1 activity and activation of its downstream modulator, PAK1. KSHV-infected endothelial cells exhibited increased phosphorylation of VE-cadherin and β-catenin, which likely contribute to the disruption of endothelial cell junctions. Consistent with these biomolecular markers, we found that latent KSHV-infected endothelial cells were more permeable than uninfected endothelial cells and that the KSHV K1 protein can induce Rac1 activation. Knockdown of Rac1 or inhibition of ROS resulted in decreased permeability in the KSHV-infected endothelial cells, suggesting that ROS and Rac1 are important mediators of KSHV-driven vascular permeability.

Methods

Cell culture

KSHV-infected human umbilical vein endothelial cells (KSHV-HUVEC) were made by infecting immortalized HUVEC with recombinant KSHV virus, as described previously.[29] HUVEC and KSHV-HUVEC were cultured in endothelial growth medium (EGM-2; Clonetics), whereas the KSHV-HUVEC were also cultured in the presence of 0.5 μg/mL of puromycin.

Reagents and antibodies

N-acetyl cysteine was purchased from Sigma-Aldrich. DPI (diphenyleneiodonium) was obtained from Calbiochem. VE-cadherin and p120 catenin antibodies were obtained from Santa Cruz Biotechnology, and the phospho-specific VE-cadherin antibodies were from BioSource International. The antibody against Rac1 was from BD Biosciences and the anti–Rac1-GTP antibody was purchased from NewEast Biosciences. The β-catenin PY654 antibody was purchased from Abcam. The mAb anti-phosphotyrosine (clone 4G10) was obtained from Upstate Biotechnology. Anti-PAK1 was obtained from Cell Signaling Technology.

siRNA and adenoviral infections

Short, interfering RNAs (siRNAs) were purchased from the UNC Nucleic Acid Core Facility/Sigma-Genosys (Sigma-Aldrich). The following siRNAs were used in this study: negative control siRNA (Guide strand 5′-UCACUCGUGCCGCAUUUCCUU-3′), Rac1 siRNA (guide strand 5′-AAACUCGCUAUGAAAUCACUU-3′). siRNAs were transfected with Lipofectamine RNAiMAX in 1 mL of Opti-MEM (Invitrogen).

Adenoviral infection was performed with WT and VE-cadherin mutants. WT VE-cadherin, VE-cadherin Y658F, VE-cadherin Y731F, and VE-cadherin Y658F/Y731F were generated as described previously.[30] Endothelial cells were infected with adenovirus for 48 hours before harvest.

Dextran flux assay

Endothelial cells were grown to confluence for a minimum of 3 days in the top well of a Transwell filter (0.4-μm, 12-mm diameter; Corning). Tetramethylrhodamine dextran (10 or 40 kDa; Molecular Probes) was added to the top chamber of the Transwell for a final concentration of 1 mg/mL. After 6 hours, the sample was removed from the bottom compartment and read in a fluorometer (FLUOStar OPTIMA; BMG Labtech) at an excitation of 555 nm and an emission of 580 nm.

Immunofluorescence and immunohistochemistry

Cells were grown on collagen-coated coverslips. Cells were fixed for 15 minutes in 4% formaldehyde, permeabilized in 0.3% Triton X-100 for 10 minutes, and blocked for 10 minutes in 5% BSA. Immunofluorescence images were taken with a Zeiss Axiovert 200M microscope equipped with a Hamamatsu ORCA-ERAG digital camera and Metamorph workstation (Universal Imaging).

For immunohistochemistry, telomerase-immortalized human umbilical vein endothelial (TIVE) tumors from mice were excised, fixed in 10% neutral-buffered formalin, paraffin embedded, and 5-μm sections were prepared on slides. In addition, normal human skin slides were obtained from US Biomax and KS tissue slides were obtained from AIDS and Cancer Specimen Resource. Slides were deparaffinized using Histochoice clearing agent (Sigma-Aldrich) and rehydrated using graded ethanol, followed by extensive washing with water. Endogenous peroxidase activity was quenched with 3% H_2O_2 in 10% methanol solution, and antigens were exposed by heating sections for 15 minutes in 1mM EDTA (pH 8.0), and cooled to room temperature. Nonspecific antigens were blocked using a blocking buffer (10% normal horse serum [Vector Labs], 5% BSA [Sigma-Aldrich], and 0.3% Triton X-100]) for 30 minutes at room temperature, followed by an overnight incubation at 4°C in PBS containing anti–active Rac1-GTP antibody (1:100; NewEast Biosciences). Sections incubated with normal mouse IgG were used as negative controls. The next day, sections were washed in PBS, incubated with biotinylated horse anti–mouse secondary antibody, followed by 1-hour incubation in preformed Avidin DH-biotinylated horseradish peroxidase H complexes (Vectastain ABC kit; Vector Laboratories), after which sections were stained with Vector NovaRed substrate and washed. Sections were counterstained with hematoxylin (Invitrogen), dehydrated using graded alcohols, and mounted using Cytoseal XYL (Richard-Allan Scientific). Dried slides were imaged using a Leica DM LA histology microscope with a 10×/0.25 numeric aperture or 40×/0.75 numeric aperture objective using a Leica DPC 480 camera and associated Leica Firecam Version 3 software on a Macintosh computer equipped with OS X10.4.

For GFP/RFP immunofluorescence, 6.25×10^5 HUVEC and KSHV-HUVEC were plated in 1 well of a 6-well dish. Images were taken with a Nikon TiE fluorescence microscope.

Immunoprecipitation

Cells were extracted on ice for 30 minutes in lysis buffer (20mM Tris pH 7.4, 150mM NaCl, 1% NP40 plus protease and tyrosine phosphatase inhibitors). Lysates were incubated with antibodies against VE-cadherin or β-catenin (4 μg) for 4 hours at 4°C. Lysates were then incubated with protein G-Sepharose beads and washed 3 times with lysis buffer. For the ROS inhibition and NADPH oxidase inhibition experiments, cells were treated with N-acetyl-cysteine (NAC; 500μM for 2 hours) or DPI (0.5μM or 2μM for 2 hours), respectively, before lysis.

Rac1 activity assays

Cells were washed with ice-cold PBS and lysed in 400 μL of buffer containing 0.5% NP-40, 50mM Tris (pH 7.0), 500mM NaCl, 1mM $MgCl_2$, 1mM EGTA, 1mM PMSF, 1 μg/mL of aprotinin, and 1 μg/mL of leupeptin. Insoluble material was removed by centrifugation for 10 minutes at 9500*g*, and the lysates were incubated for 30 minutes with 50 μg of immobilized glutathione S-transferase-p21–binding domain (GST-PBD) at 4°C to measure Rac1 activity.[31] For the assay in HEK293 cells, 8 μg of Flag epitope-tagged pcDNA3-K1 or pcDNA3 vector was transfected into HEK293 cells using Lipofectamine 2000. After transfection, the cells were serum starved for 48 hours. Cells were harvested and lysed as described earlier in this paragraph, and 500 μg of cell lysate was used per immunoprecipitation along with 1 μg of anti–Rac1-GTP antibody. The immunoprecipitations were performed at 4°C for 14 hours, after which time the immunoprecipitates were washed and loaded on SDS-PAGE. The samples were then subjected to Western blot analysis with an anti-Rac1 antibody.

PAK1 kinase assay

PAK1 kinase assay was performed as described by Knaus et al.[32] Cells were plated in 100-mm dishes. When confluent, cells were washed with PBS twice and harvested. Cells were centrifuged at 1250*g* for 10 minutes, 400 μL of cold lysis buffer (1% NP-40, 50mM Tris-HCl, pH 8.0, and 150mM NaCl) was added, and the samples were incubated on ice for 30 minutes. The lysates were sonicated and the samples were spun at 17 000*g* at 4°C. The supernatants were harvested and 500 μg of lysate in 500 μL of lysis buffer was mixed with 6 μL of anti-PAK1 antibody and incubated at 4°C for 2 hours. After incubation, 25 μL of protein A/G plus-agarose (Santa Cruz Biotechnology) was added, and samples were nutated at 4°C overnight, washed in lysis buffer (50mM HEPES, pH7.5, 10mM $MgCl_2$, 2mM $MnCl_2$, and 0.2mM DTT) and 13 μL of kinase buffer containing 2 μg of myelin binding protein (MBP) substrate, 20μM cold ATP, and 5 μCi of γ-^{32}P ATP (3000 Ci/mmol, 10mCi/mL; PerkinElmer) was mixed with 12.5 μL of immunoprecipitation beads, and the mixture was incubated at 30°C for 20 minutes. The samples were then subjected to SDS-PAGE. The gel was dried and exposed to film. The Rac1 knockdown was performed as described in "Rac1 activity assays" before harvest for the kinase assay. For the ROS inhibition experiment, confluent cells were treated with 500μM of *N*-acetyl-cysteine (final concentration) for 2 hours before harvest for the kinase assay.

Src kinase activity assay

Confluent cells were washed in PBS and lysed in 400 μL of cold lysis buffer (1% NP-40, 50mM Tris-Cl pH 8.0, NS 150mM NaCl). Lysates were centrifuged and 500 μg of lysate was used for immunoprecipitation with 3 μg of anti-Src antibody (clone GD11; Millipore). Next, 20 μL of Protein A/G plus-Agarose beads was added to the lysate and the complexes were allowed to bind at 4°C overnight. The beads were washed with lysis buffer 3 times, followed by 2 washes with kinase buffer (50mM HEPES, 150mM NaCl, 5mM MgCl,10mM NaF, and 1mM Na_3VO_4). Src kinase assays were performed as per the manufacturer's instruction (Src Assay Kit; Millipore). The kinase reaction solution (25 μL) was spotted onto P81 filter paper, the filter was washed with 0.75% phosphoric acid 5 times and once with acetone, and then the filter was transferred to a vial for counting with a scintillation counter.

Scratch assay

HUVEC and KSHV-HUVEC (8×10^5) were seeded in 1 well of a 6-well dish. Cells were scratched with a P10 pipette tip 24 hours later. Cells were imaged at 0, 6, and 12 hours. The percentage of gap filled with migrated cells at 6 hours was calculated by measuring the space filled by cells at 6 hours and normalizing to the gap measured at 0 hours.

PCR of viral genes

Primer sets used to detect viral gene expression were as follows. vGPCR primers: 5′-GTGCCTTACACGTGGAACGTT-3′and 5′-GGTGACCAATC-CATTTCCAAGA-3′. Rta primers: 5′-CCCTGAGCCAGTTTGTCATT-3′ and 5′-ATGGGTTAAAGGGGATGATG-3′. Latency-associated nuclear antigen (LANA/Orf73) primers: 5′-CGCGAATACCGCTATGTACTCA-3′ and 5′-GGAACGCGCCTCATACGA-3′. K1 primers: 5′-CCAAACGGAC-GAAATGAAAC-3′ and 5′-TGTGTGGTTGCATCGCTATT-3′. Human GAPDH primers: 5′-GAAGGTGAAGGTCGGAGT-3′ and 5′-GAAGA-TGGTGATGGGATTTC-3′.

For viral gene-expression analysis, 2×10^6 cells of HUVEC, KSHV-HUVEC, and reactivated KSHV-293 cells (positive control) were harvested. Total RNA was extracted using the QIAGEN RNeasy Plus Kit. RNA was treated with DNase for 1 hour at 37°C and then repurified with the RNeasy Plus kit; 1 μg of each RNA sample was used for cDNA synthesis with M-MLV Reserve Transcriptase (Invitrogen), 1 μL of cDNA sample was subjected to PCR, and the products were electrophoresed on an agarose gel.

VEGF quantitation

HUVEC and KSHV-HUVEC (6.25×10^5) were seeded in 1 well of a 6-well dish. Twenty-four hours later, cells were washed twice with PBS, and 3 mL of 2% FBS medium without supplements was added. The supernatants were harvested at 48 hours and subjected to Luminex profiling using the human 15-plex Luminex kit (Millipore).

Results

Rac1 is activated in latent KSHV-infected endothelial cells

We reported previously the generation of KSHV-infected HUVEC using the rKSHV.219 strain of KSHV, which expresses green fluorescent protein (GFP) under a EF-1α promoter and red fluorescent protein (RFP) under the promoter for the viral lytic gene PAN.[33] The KSHV-infected cells are highly latent and only express GFP and not RFP (supplemental Figure 1A, available on the *Blood* Web site; see the Supplemental Materials link at the top of the online article). In addition, using PCR to detect viral gene expression, we were able to detect expression of both LANA/Orf73 and K1 in the KSHV-HUVEC (supplemental Figure 1B). This result is consistent with other reports from Ganem et al showing that K1 is transcribed in latent KSHV-infected cells, including tightly latent infected endothelial cells.[28] Although we did not find expression of the lytic gene RTA (supplemental Figure 1B), we cannot rule out the possibility that there was still some lytic gene expression that was below the level of detection of our RT-PCR.

We and others have reported previously that KSHV-infected endothelial cells up-regulate VEGF expression and secretion.[29,34] We found that KSHV-HUVEC secrete approximately 4 times as much VEGF into the supernatant than uninfected HUVEC (Figure 1A). To determine whether latent KSHV infection affects Rac1 activity in endothelial cells, we used latent KSHV-infected human umbilical vein endothelial cells (KSHV-HUVEC) and uninfected HUVEC which have been described previously.[29] We assessed Rac1 activation using a Rac1-GTP pull-down assay with GST-PBD. The latent KSHV-HUVEC displayed high levels of Rac1 activity compared with uninfected cells (Figure 1B). Similar results were obtained using immunoprecipitation of activated Rac1-GTP (Figure 1C) from uninfected and KSHV-infected HUVEC. Src kinase activation is known to lead to the activation of Rac1,[35] so we performed a Src kinase activity assay in uninfected and latent KSHV-infected endothelial cells. We found that the latent KSHV-infected endothelial cells displayed increased Src kinase activity (Figure 1D). Rac1 activation has also been shown previously to be correlated with activation of PAK1.[6,36,37] Therefore, we also analyzed the activity of PAK1 by performing an immunoprecipitation with PAK1 antibody, followed by an in vitro kinase assay using MBP as a substrate. We found that PAK1 was more activated in the latent KSHV-infected endothelial cells (Figure 1E).

Latent KSHV infection increases VE-cadherin and β-catenin phosphorylation

Rac1 is known to regulate tyrosine phosphorylation of several junctional proteins, including VE-cadherin and β-catenin.[6,9,38,39] To determine whether latent KSHV infection affects VE-cadherin tyrosine phosphorylation, VE-cadherin was immunoprecipitated and the total phosphotyrosine level was analyzed. As shown in Figure 2A, latent infection with KSHV increased the phosphorylation of VE-cadherin in endothelial cells. Phosphorylation of VE-cadherin at Tyr-658 and Tyr-731 has been shown previously to affect junctional integrity through inhibition of p120-catenin and β-catenin binding.[40] Therefore, we measured VE-cadherin phosphorylation at Tyr-658 and Tyr-731. The latent KSHV-HUVEC displayed increased phosphorylation of both of these tyrosine residues

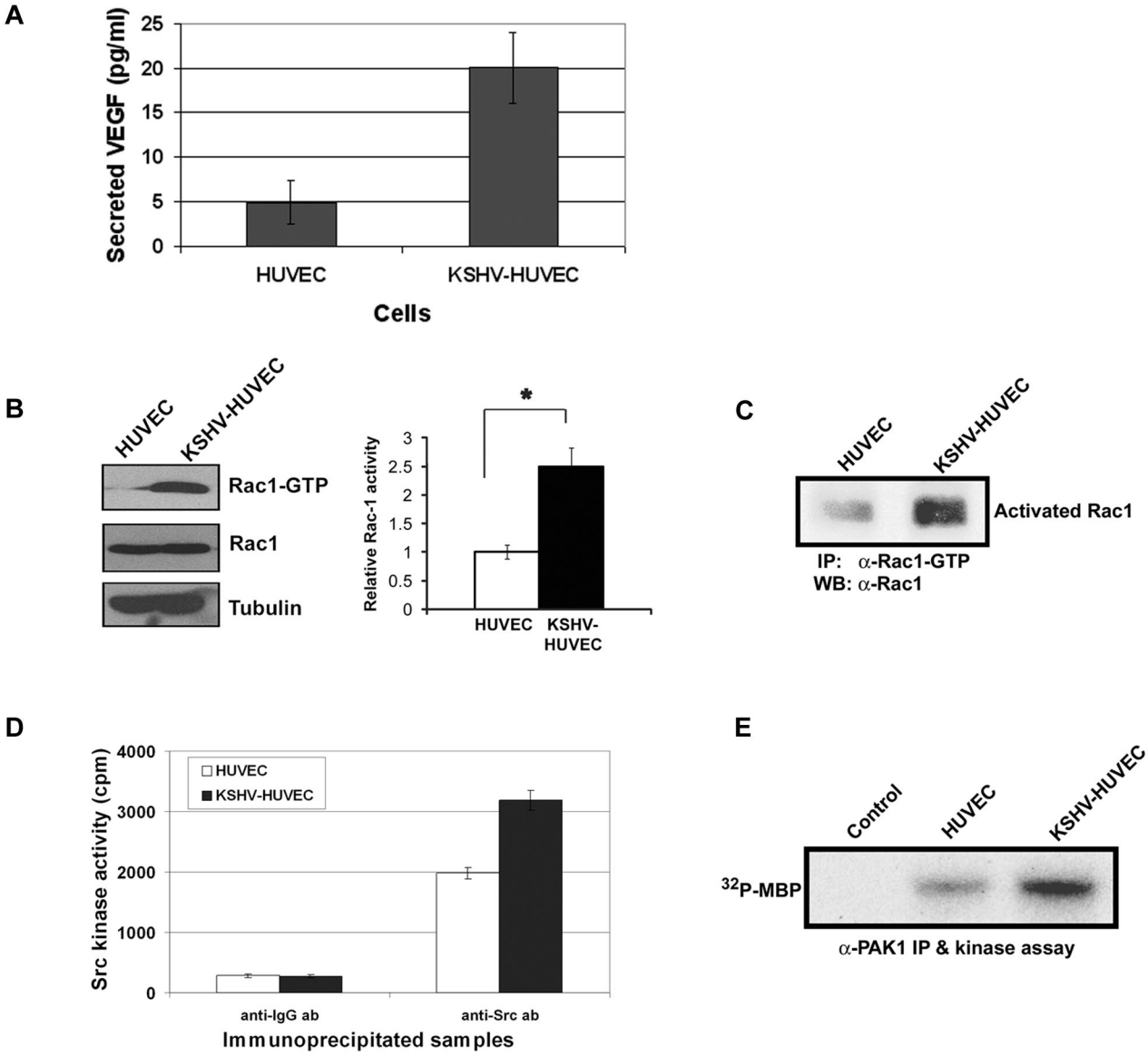

Figure 1. Rac1 is activated in KSHV-infected endothelial cells. (A) The amount of VEGF secreted from uninfected HUVEC and KSHV-infected HUVEC was determined by Luminex assay (Millipore). Four individual replicates were performed and the error bars represent the SD. (B) Detection of activated Rac1 in HUVEC and KSHV-HUVEC. HUVEC and KSHV-HUVEC were harvested, lysed, and activated Rac1 (Rac1-GTP) was immunoprecipitated with GST-PBD and analyzed by Western blot analysis. Corresponding densitometric analysis of Rac1-GTP normalized to Rac1 levels was performed, and this is shown as relative Rac1 activity in the HUVEC. Values are presented as the mean ± SD of 5 independent experiments. $^*P < .05$; n = 5. (C) HUVEC and KSHV-HUVEC were grown to confluence and the cell lysates were immunoprecipitated with anti–Rac1-GTP antibody. The immunoprecipitates were subjected to Western blot analysis with anti-Rac1 antibody. The level of activated Rac1 in KSHV-HUVEC was higher than that in HUVEC. (D) Increased Src kinase activity was observed in KSHV HUVEC compared with HUVEC. Cell lysates from both cells were immunoprecipitated with anti-Src antibody (clone GD11; Millipore). Src kinase assays were performed as per the manufacturer's instructions. Anti-Src immunoprecipitations were used in a kinase assay with the KVEKIGEGTYGVVYK peptide as substrate. Immunoprecipitated complexes with normal mouse IgG were used as the negative control. Phosphorylated peptide was quantitated using a scintillation counter. Values are presented as the mean ± SD of 4 independent experiments. (E) Increased PAK1 kinase activity was seen in KSHV-HUVEC compared with HUVEC.PAK1 immunoprecipitated from cell lysates were used in the kinase assays, along with MBP as the PAK1 substrate. Samples were subjected to SDS-PAGE. ^{32}P-labeled MBP was visualized by autoradiography.

of VE-cadherin (Figure 2B), but the total level of VE-cadherin was unchanged in both cell lines. Interestingly, similar results were observed when β-catenin phosphorylation was examined. Indeed, immunoprecipitation of β-catenin followed by immunoblotting with an anti-phosphotyrosine antibody revealed enhanced tyrosine phosphorylation of β-catenin in latent KSHV-infected endothelial cells (Figure 2C). However, similar to VE-cadherin, total levels of β-catenin were not changed (Figure 2C-D). Similarly, examination of β-catenin at Tyr-654 also revealed elevated phosphorylation in latent KSHV-HUVEC compared with uninfected HUVEC (Figure 2D).

Rac1 is necessary for KSHV-induced VE-cadherin and β-catenin phosphorylation

To determine whether Rac1 contributes to the increase in VE-cadherin and β-catenin phosphorylation observed in latent KSHV-infected endothelial cells, we depleted Rac1 expression using siRNA. Depletion of Rac1 greatly decreased VE-cadherin phosphorylation on tyrosine in KSHV-HUVEC (Figure 3A) to a level similar to that observed in uninfected endothelial cells. In addition, phosphorylation at Tyr-731 was decreased upon depletion of Rac1 in latent KSHV-HUVEC. To further examine the effect of Rac1

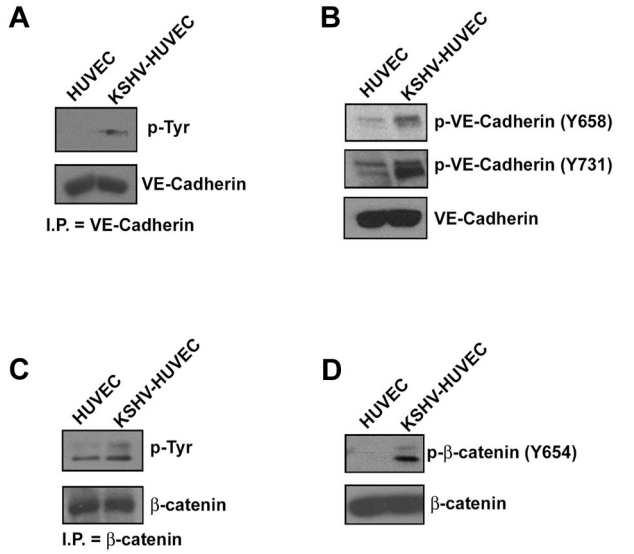

Figure 2. KSHV infection increases VE-cadherin and β-catenin phosphorylation. (A) VE-cadherin was immunoprecipitated with anti–VE-cadherin antibody from lysates of HUVEC and KSHV-HUVEC and analyzed by Western blot using anti-phosphotyrosine antibody (clone 4G10). (B) HUVEC and KSHV-HUVEC lysates were analyzed by Western blot for phosphorylated forms of VE-cadherin using antibodies that specifically recognize VE-cadherin phosphorylated at Tyr-658 (Y658) and Tyr-731 (Y731). Total VE-cadherin was used as a loading control. (C) β-catenin was immunoprecipitated with anti–β-catenin antibody from lysates of HUVEC and KSHV-HUVEC, and analyzed by Western blot using anti-phosphotyrosine antibody (clone 4G10). (D) HUVEC and KSHV-HUVEC lysates were analyzed by Western blot for phosphorylated forms of β-catenin using antibodies that specifically recognize β-catenin phosphorylated at Tyr-654 (Y654). Total β-catenin was used as a loading control.

knockdown on the phosphorylation of junctional proteins, we also analyzed β-catenin phosphorylation. Rac1 knockdown reduced total tyrosine phosphorylation as well as phosphorylation at Tyr-654 of β-catenin in KSHV-HUVEC (Figure 3B). These data demonstrate that Rac1 is required for the KSHV-induced phosphorylation of VE-cadherin and β-catenin.

Latent KSHV infection affects junctional integrity

Tyrosine phosphorylation of junctional proteins is indicative of decreased junctional integrity. To further explore junctional integrity during latent KSHV infection, we examined VE-cadherin and β-catenin localization (Figure 4A-B). As can be seen in the magnified area in Figure 4A, there appears to be interrupted VE-cadherin staining in KSHV-HUVEC compared with uninfected HUVEC. In KSHV-infected endothelial cells, VE-cadherin and β-catenin staining were moderately altered, displaying irregular and jagged junctions. In addition, immunofluorescence staining of KSHV-infected endothelial cells showed highly activated Rac1-GTP compared with uninfected cells (Figure 4C).

Latent KSHV infection increases endothelial permeability in a Rac1-dependent manner

To determine whether the junctional dysregulation observed in latent KSHV-infected endothelial cells affects endothelial cell permeability, we used a FITC-dextran Transwell assay. KSHV-HUVEC or uninfected HUVEC were grown to confluence on Transwell filters and rhodamine-dextran was added. We found that KSHV-infected endothelial cells were much more permeable to 10-kDa dextran (Figure 5A). An increase in permeability of the KSHV-infected endothelial cells was also observed with 40-kDa dextran (Figure 5B).

To determine whether Rac1 contributes to the increase in permeability observed in KSHV-HUVEC, we knocked down Rac1 using siRNA. As shown in Figure 5C, depletion of Rac1 abrogated the permeability of KSHV-HUVEC cells to 10-kDa dextran. Because we demonstrated that latent infection with KSHV increases VE-cadherin phosphorylation in a Rac1-dependent manner (Figure 3A), we next sought to determine whether VE-cadherin phosphorylation was critical for the ability of KSHV to enhance vascular permeability. WT VE-cadherin or a double mutant in which both Tyr-658 and Tyr-731 had been mutated to phenylalanines (YY/FF) was transfected into the HUVEC and KSHV-HUVEC. We found that KSHV infection increased vascular permeability in endothelial cells expressing WT VE-cadherin (Figure 5D). However, expression of the phosphorylation-resistant double mutant of VE-cadherin (YY/FF) reduced the effect of KSHV infection on endothelial cell permeability (Figure 5D). These results demonstrate that latent KSHV infection increases

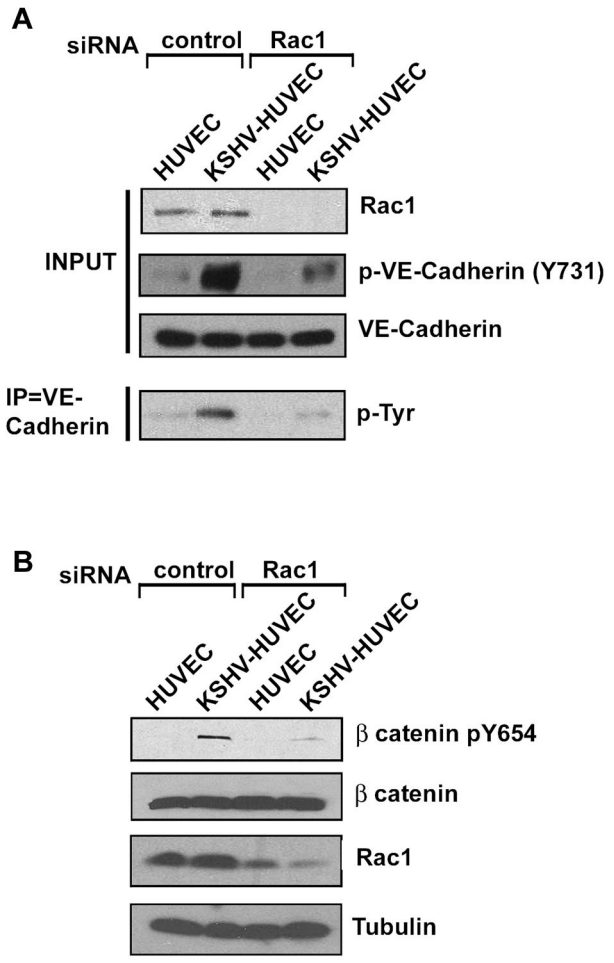

Figure 3. Rac1 is necessary for KSHV-induced VE-cadherin and β-catenin phosphorylation. (A) HUVEC and KSHV-HUVEC were transfected for 48 hours with control siRNA or siRNA targeting Rac1 and then lysed. VE-cadherin was immunoprecipitated with anti–VE-cadherin antibody and analyzed by Western blot using anti-phosphotyrosine antibody (clone 4G10). The phosphorylated forms of VE-cadherin were analyzed by immunoblotting using antibodies that specifically recognize VE-cadherin phosphorylated at Tyr-731 (Y731). Total VE-cadherin was used as a loading control. (B) HUVEC and KSHV-HUVEC were transfected for 48 hours with control siRNA or siRNA targeting Rac1 and then lysed. Lysates were analyzed by Western blot for phosphorylated forms of β-catenin using antibodies that specifically recognize β-catenin phosphorylated at Tyr-654 (Y654). Total β-catenin was used as a loading control.

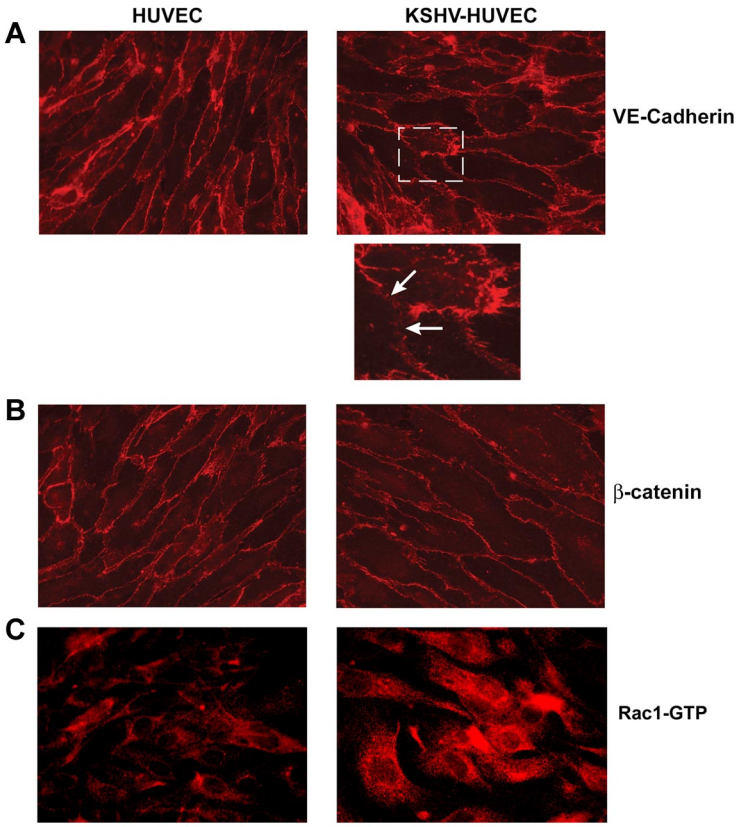

Figure 4. KSHV latent infection affects junctional integrity. HUVEC and KSHV-HUVEC were grown on coverslips, fixed, permeabilized, and stained with an antibody against VE-cadherin (A), β-catenin (B), and Rac1-GTP (C). Magnification, ×63, oil-immersion microscope. Bottom of panel A shows magnification (2.5×) of white box inset.

vascular permeability through Rac1-mediated phosphorylation of VE-cadherin.

Defects in cell-cell adhesion junctions can affect the capacity of cells to migrate collectively[41] and increases in activated Rac1 can increase migratory ability. We investigated whether KSHV infection affected endothelial cell migration by performing a scratch assay. Briefly, HUVEC and KSHV-HUVEC were plated and grown to confluence. The cell monolayer was scratched using a pipette tip and the ability of the cells to grow back into a monolayer was measured at 0, 6, and 12 hours. Figure 5E-F shows that the KSHV-HUVEC grew back approximately twice as fast as the uninfected cells.

KSHV-induced endothelial permeability requires ROS production

We demonstrated recently that Rac1 regulates VE-cadherin tyrosine phosphorylation through the generation of ROS.[9,10] To determine whether ROS production contributes to KSHV-induced VE-cadherin phosphorylation, we used the free radical scavenger NAC. We found that treatment with NAC inhibited the KSHV-induced increase in VE-cadherin phosphorylation (Figure 6A). To further examine the role of ROS in the KSHV-mediated increase in vascular permeability, KSHV-HUVEC and uninfected HUVEC were grown to confluence on Transwell filters and treated with NAC. As expected, NAC abrogated the effect of KSHV infection on endothelial permeability to 10-kDa dextran (Figure 6B). Knockdown of Rac1 also reduced PAK1 kinase activity in latent KSHV-HUVEC, and treatment with the ROS scavenger NAC dramatically reduced PAK1 activation in these cells (Figure 6C). To determine whether NADPH oxidase was the main source of ROS responsible for the endothelial permeability, we treated cells with 0, 0.5, or 2μM of a NADPH oxidase inhibitor, DPI, as described previously.[9] We found that both concentrations of DPI significantly reduced the tyrosine phosphorylation of VE-cadherin (Figure 6D), suggesting that NADPH oxidase is the primary source for the generation of ROS and induction of vascular permeability in the KSHV-infected endothelial cells.

In an effort to determine which viral protein expressed in the latently infected KSHV-HUVEC could activate Rac1, we investigated whether the KSHV K1 protein could activate Rac1. The reason for examining K1 specifically was because it had been reported previously that K1 can induce VEGF expression and VEGF-VEGFR signaling in endothelial cells[26,42] and therefore it seemed to be a likely candidate. In addition, as supplemental Figure 1B shows, K1 is transcribed in KSHV-HUVEC, which is consistent with a recent report from Chandriani et al and our previous report showing K1 is expressed in KS tumors in the absence of the lytic gene Rta.[26,28] To determine whether K1 was able to activate Rac1, HEK293 cells were transfected with either pcDNA3 vector alone or pcDNA3-K1, and 48 hours after transfection, cells were harvested and subjected to immunoprecipitation with anti–Rac1-GTP antibody followed by Western blotting for Rac1 antibody. In 3 independent experiments, we found that the expression of K1 increased Rac1 activation (Figure 7A).

Finally, to determine whether activated Rac1 is present in KSHV-infected tumors, we injected nude mice with 1×10^6 TIVE cells,[43] KSHV-infected endothelial cells that have been previously reported to form tumors in immunodeficient mice.[43] Tumors were harvested, sectioned, and immunohistochemistry was performed with normal mouse IgG as a control antibody or an anti–Rac1-GTP antibody that specifically detects the activated form of Rac1. As can be seen in Figure 7B, KSHV-infected endothelial cell tumors

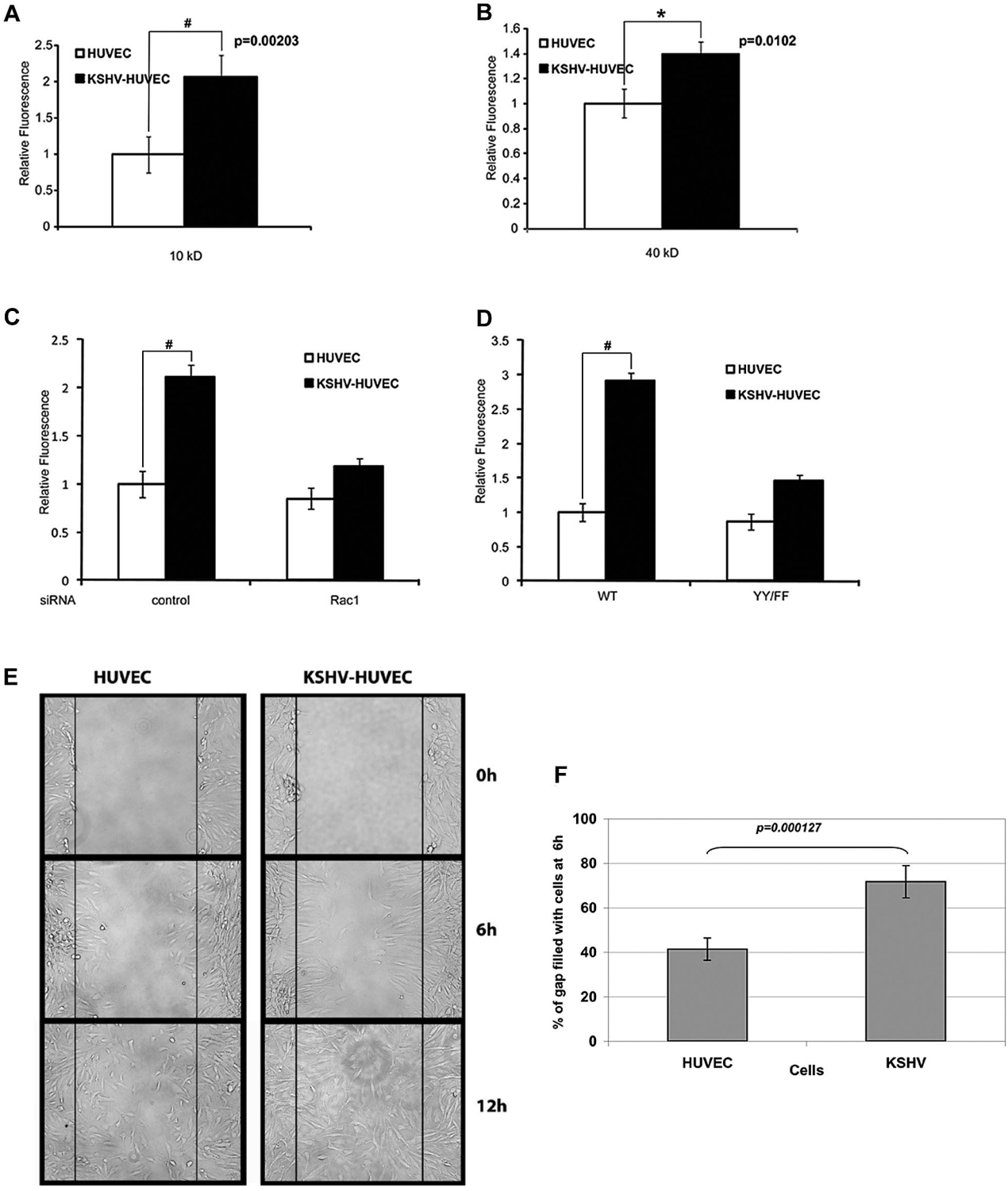

Figure 5. KSHV infection increases endothelial permeability in a Rac1-dependent manner. (A) HUVEC and KSHV-HUVEC were seeded in the upper well of a Transwell chamber and allowed to grow to confluence. FITC-dextran (10 kDa) was placed in the upper well. A sample of medium from the lower chamber was taken after 6 hours, and the amount of FITC-dextran in the lower chamber was measured in a plate reader. These are representative graphs of triplicate assays (#$P < .01$). (B) HUVEC and KSHV-HUVEC were seeded in the upper well of a Transwell chamber and allowed to grow to confluence. FITC-dextran (40 kDa) was placed in the upper well. A sample of medium from the lower chamber was taken after 6 hours, and the amount of FITC-dextran in the lower chamber was measured in a plate reader. These are representative graphs of triplicate assays (*$P < .05$). (C) HUVEC and KSHV-HUVEC were transfected for 48 hours with control siRNA or siRNA targeting Rac1 and then seeded in the upper well of a Transwell chamber and allowed to grow to confluence. FITC-dextran (10 kDa) was placed in the upper well. The amount of FITC-dextran in the lower chamber was measured in a plate reader 6 hours later. These are representative graphs of triplicate assays (#$P < .01$). (D) HUVEC and KSHV-HUVEC were infected with adenovirus containing WT VE-cadherin or a phosphorylation-resistant mutant of VE-cadherin (YY/FF), and then seeded in the upper well of a Transwell chamber and allowed to grow to confluence. FITC-dextran (10 kDa) was placed in the upper well. The amount of FITC-dextran in the lower chamber was measured in a plate reader 6 hours later. These are representative graphs of triplicate assays (#$P < .01$). (E) KSHV-HUVEC display increased migratory potential. HUVEC and KSHV-HUVEC were seeded in 1 well of a 6-well dish for 24 hours. After wound formation (with a P10 pipette tip), cells were imaged at 0, 6, and 12 hours. (F) The percentage of the gap filled with migrated cells at 6 hours was normalized to the gap measured at 0 hours. The measurements were averaged from 10 different experiments. Error bars represent SD.

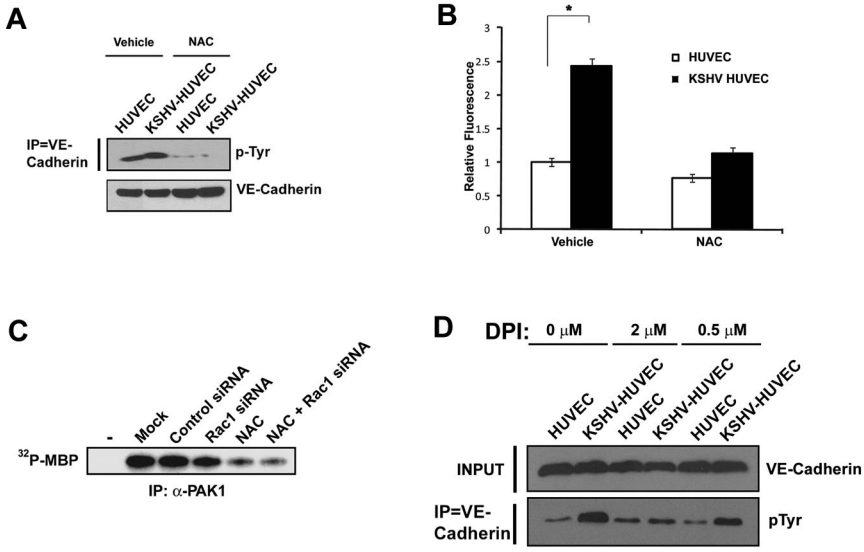

Figure 6. KSHV-induced endothelial permeability requires ROS production. (A) HUVEC and KSHV-HUVEC were treated with NAC (500μM) or vehicle control for 2 hours. VE-cadherin was immunoprecipitated and the immunoprecipitates were subjected to immunoblot analysis with an anti-phosphotyrosine antibody (clone 4G10). (B) HUVEC and KSHV-HUVEC were seeded in the upper well of a Transwell chamber and allowed to grow to confluence. After a 2-hour treatment with NAC (500μM), FITC-dextran (10 kDa) was placed in the upper well. The amount of FITC-dextran in the lower chamber was measured in a plate reader 6 hours later ($P < .01$; $n = 3$). (C) Rac1 and ROS affect PAK1 activity. Rac1 siRNA was transfected into KSHV-HUVEC. Cells were harvested 72 hours after transfection. Cells were treated with NAC for 2 hours before harvest. Cell lysates were subjected to immunoprecipitation with an anti-PAK1 antibody and kinase assays were performed. Rac1 siRNA transfected cells showed lower PAK1 kinase activity compared with control siRNA-transfected cells. In addition, NAC-treated KSHV-HUVEC and NAC treatment of Rac1 siRNA–transfected cells displayed the lowest level of PAK1 kinase activity. (D) HUVEC and KSHV-HUVEC were treated with DPI (0.5μM or 2μM) or vehicle control for 2 hours. VE-cadherin was immunoprecipitated and the immunoprecipitates were subjected to immunoblot analysis with an anti-phosphotyrosine antibody (clone 4G10).

display high levels of activated Rac1 protein. We also stained normal skin (Figure 7C) and KS tissue sections from 2 different donors (Figure 7D) and found that both KS tumor sections displayed increased amounts of activated Rac1-GTP compared with normal skin.

Discussion

The majority of cells in the KS lesion are latently infected with KSHV, but not much is known about the effects of latent KSHV infection on endothelial cell permeability. Studies assessing endothelial cell permeability have only been performed in the context of KSHV lytic infection. These studies showed that lytic infection leads to the degradation of VE-cadherin in endothelial cells[44] and that the KSHV K5 and vGPCR lytic viral proteins may be responsible for this effect.[45,46] KSHV lytic infection of endothelial cells resulted in the down-regulation of VE-cadherin protein levels by 4 hours after infection.[44] In addition, KSHV K5 was specifically shown to target VE-cadherin for ubiquitin-mediated destruction, resulting in lower protein levels of VE-cadherin in the presence of KSHV K5.[45]

Because the majority of the KS lesion is composed of latently infected endothelial cells, we examined Rac1 activation and endothelial cell permeability in the context of viral latency. We found that, similar to lytic infection, latent KSHV infection of endothelial cells also results in the disruption of endothelial cell junctions, albeit through an independent and completely different mechanism. We found that the KSHV K1 is transcribed in the latently infected endothelial cells, a finding similar to other reports,[26,28] and now demonstrate that K1 can activate Rac1. It is possible that other latent viral proteins may also contribute to Rac1 activation. Although the total levels of VE-cadherin remained equal in uninfected and latently infected endothelial cells, the tyrosine phosphorylation levels of VE-cadherin in latently infected cells was greatly increased. This suggests that during latent infection, KSHV activates signal transduction pathways that lead to the tyrosine phosphorylation of VE-cadherin, resulting in endothelial cell disruption. We found an increase in Src kinase activity and activated Rac1 in KSHV-infected endothelial cells compared with uninfected cells. PAK1, a downstream target of activated Rac1, was also activated in the KSHV-infected cells compared with the uninfected cells. These data are corroborated by the fact that both KSHV-infected endothelial cell tumors generated in nude mice and KS tumors display high levels of Rac1-GTP.

We found that activated Rac1 was required for the increased phosphorylation of VE-cadherin and β-catenin in KSHV-infected cells and for the increased permeability of the KSHV-infected endothelial cells, because Rac1 knockdown reduced the phosphorylation of both VE-cadherin and β-catenin and also reduced cell permeability. The activation of Src and Rac1 have been shown to result in increased ROS production.[9,10] Treatment with the ROS inhibitor NAC reduced VE-cadherin phosphorylation levels and KSHV-induced vascular permeability. NADPH oxidase is a major source of ROS in endothelial cells[47] and Rac1 is known to regulate NADPH activity.[9,47] Consistent with this, we found that NADPH oxidase inhibition decreased VE-cadherin phosphorylation in the infected cells, indicating that NADPH oxidase activation mainly contributes to Rac1-mediated ROS production in latently infected endothelial cells.

Other investigators have shown that the KSHV lytic vGPCR protein can affect Rho protein activity[25,45,46,48,49] and activate VEGF and Rac1.[24,25,49] In the present study, we show that KSHV K1 can also activate Rac1. This suggests that both KSHV latent and lytic viral proteins expressed in KS tumors synergize to up-regulate Rac1 signaling and increase vascular permeability. The virus needs both lytic and latent genes for its survival and pathogenesis. Without lytic genes, the virus cannot replicate and exert paracrine

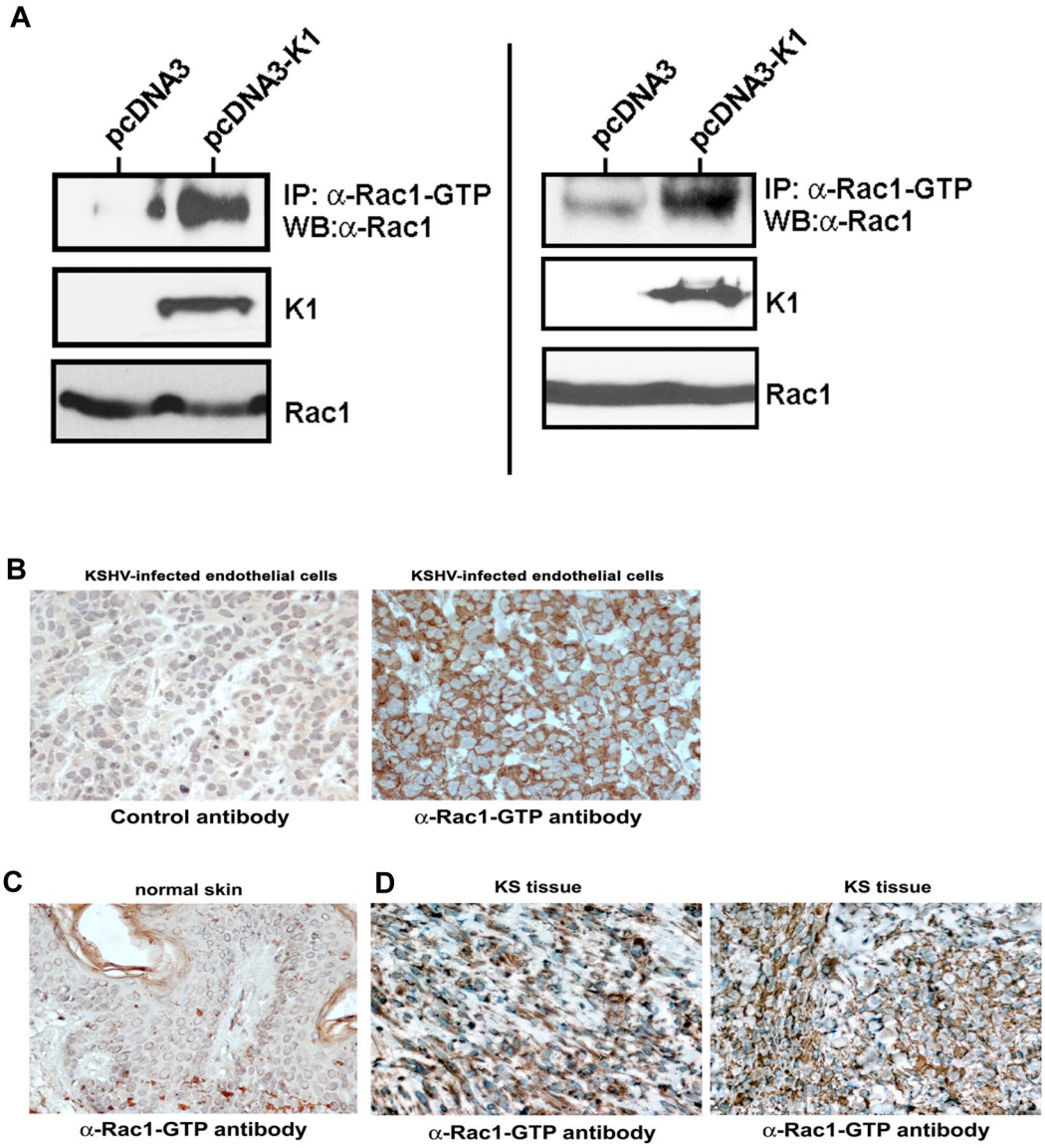

Figure 7. Rac1 is activated in K1-expressing cells and in KS tumors. (A) HEK293 cells were transfected with either pcDNA3 vector alone or pcDNA3-K1 and 48 hours after transfection, cells were harvested and subjected to immunoprecipitation with anti–Rac1-GTP antibody followed by Western blotting for Rac1. Two independent anti–Rac1-GTP immunoprecipitations from vector and K1-expressing cells are shown. Expression of K1 and Rac1 in these cells was verified by Western blot. (B) Immunohistochemistry showing active Rac1-GTP in tumor sections from mice injected with KSHV-infected endothelial cells. (C) Immunohistochemistry showing active Rac1-GTP in normal human skin sections. (D) Immunohistochemistry showing active Rac1-GTP in KS tumor tissue sections. No staining was observed in the presence of a control antibody (panel B). Original magnification, ×400.

effects on uninfected cells, and without latent genes, the virus cannot persist and establish latency in the infected host. Because KSHV encodes for > 100 viral genes and microRNAs combined, it is likely that both lytic and latent gene products are needed for survival of the virus and that these work in synergy.

In summary, we find that under conditions of latent infection, KSHV dramatically up-regulates the activity of Rac1, leading to endothelial junction dysregulation and increased vascular permeability. KSHV K1 is expressed in latently infected endothelial cells and can activate Rac1. Human KS tumors display prominent angiogenesis and vascular permeability, which can be attributed to the ability of the virus to up-regulate pro-angiogenic factors. Our findings correlate well with the increased vascular permeability seen in human KS tumor lesions,[50] and suggest that viral infection with KSHV is the key inducer of disrupted endothelial cell junctions. The increased vascular permeability may result from the increased secretion of VEGF from infected cells, and this may allow the virus to attract leukocytes to the site of KSHV-infected endothelial cells and help the virus to spread to other cell types such as B cells and monocytes.

Acknowledgments

The authors thank Dr Rolf Renne for providing the TIVE cells, Dr Jeff Vieira for providing the recombinant KSHV virus, and the AIDS and Cancer Specimen Resource for the KS tumor specimens. B.D. is a Leukemia & Lymphoma Society Scholar and a Burroughs Welcome Fund Investigator in Infectious Disease.

This work was supported by National Institutes of Health grants CA096500 and CA019014 to B.D. and HL080166 and GM029860 to K.B. C.G. is supported by a Marie Curie

Outgoing International Fellowship from the European Union Seventh Framework Program (FP7/2007-2013) under grant agreement number 254747.

Authorship

Contribution: C.G. and Z.Z. planned the research, performed the experiments, analyzed the data, drafted the first and subsequent drafts of the manuscript, and approved the final version of the manuscript; P.M.B., L.S., and L.W. performed the experiments; analyzed the data, assisted in the drafting of the manuscript, and approved the final version of the manuscript; and K.B. and B.D. planned the research, analyzed the data, drafted the first and subsequent drafts of the manuscript, and approved the final version of the manuscript.

Conflict-of-interest disclosure: The authors declare no competing financial interests.

Correspondence: Blossom Damania, Lineberger Comprehensive Cancer Center, CB#7295, University of North Carolina, Chapel Hill, NC 27599; e-mail: damania@med.unc.edu.

References

1. Weis SM, Cheresh DA. Pathophysiological consequences of VEGF-induced vascular permeability. *Nature.* 2005;437(7058):497-504.
2. May C, Doody JF, Abdullah R, et al. Identification of a transiently exposed VE-cadherin epitope that allows for specific targeting of an antibody to the tumor neovasculature. *Blood.* 2005;105(11): 4337-4344.
3. Fukuhara S, Sakurai A, Sano H, et al. Cyclic AMP potentiates vascular endothelial cadherin-mediated cell-cell contact to enhance endothelial barrier function through an Epac-Rap1 signaling pathway. *Mol Cell Biol.* 2005;25(1):136-146.
4. Weis S, Cui J, Barnes L, Cheresh D. Endothelial barrier disruption by VEGF-mediated Src activity potentiates tumor cell extravasation and metastasis. *J Cell Biol.* 2004;167(2):223-229.
5. Corada M, Mariotti M, Thurston G, et al. Vascular endothelial-cadherin is an important determinant of microvascular integrity in vivo. *Proc Natl Acad Sci U S A.* 1999;96(17):9815-9820.
6. Gavard J, Gutkind JS. VEGF controls endothelial-cell permeability by promoting the beta-arrestin-dependent endocytosis of VE-cadherin. *Nat Cell Biol.* 2006;8(11):1223-1234.
7. Garrett TA, Van Buul JD, Burridge K. VEGF-induced Rac1 activation in endothelial cells is regulated by the guanine nucleotide exchange factor Vav2. *Exp Cell Res.* 2007;313(15):3285-3297.
8. Stockton RA, Schaefer E, Schwartz MA. p21-activated kinase regulates endothelial permeability through modulation of contractility. *J Biol Chem.* 2004;279(45):46621-46630.
9. Monaghan-Benson E, Burridge K. The regulation of vascular endothelial growth factor-induced microvascular permeability requires Rac and reactive oxygen species. *J Biol Chem.* 2009;284(38): 25602-25611.
10. Monaghan-Benson E, Hartmann J, Vendrov AE, et al. The role of vascular endothelial growth factor-induced activation of NADPH oxidase in choroidal endothelial cells and choroidal neovascularization. *Am J Pathol.* 2010;177(4):2091-2102.
11. Boshoff C, Schulz TF, Kennedy MM, et al. Kaposi's sarcoma-associated herpesvirus infects endothelial and spindle cells. *Nat Med.* 1995; 1(12):1274-1278.
12. Humphrey RW, Davis DA, Newcomb FM, Yarchoan R. Human herpesvirus 8 (HHV-8) in the pathogenesis of Kaposi's sarcoma and other diseases. *Leuk Lymphoma.* 1998;28(3-4):255-264.
13. Dupin N, Grandadam M, Calvez V, et al. Herpesvirus-like DNA sequences in patients with Mediterranean Kaposi's sarcoma. *Lancet.* 1995; 345(8952):761-762.
14. Bernstein WB, Little RF, Wilson WH, Yarchoan R. Acquired immunodeficiency syndrome-related malignancies in the era of highly active antiretroviral therapy. *Int J Hematol.* 2006;84(1):3-11.
15. Cesarman E, Chang Y, Moore PS, Said JW, Knowles DM. Kaposi's sarcoma-associated herpesvirus-like DNA sequences in AIDS-related body-cavity-based lymphomas. *N Engl J Med.* 1995;332(18):1186-1191.
16. Soulier J, Grollet L, Oksenhendler E, et al. Kaposi's sarcoma-associated herpesvirus-like DNA sequences in multicentric Castleman's disease. *Blood.* 1995;86(4):1276-1280.
17. Dupin N, Fisher C, Kellam P, et al. Distribution of human herpesvirus-8 latently infected cells in Kaposi's sarcoma, multicentric Castleman's disease, and primary effusion lymphoma. *Proc Natl Acad Sci U S A.* 1999;96(8):4546-4551.
18. Boshoff C, Endo Y, Collins PD, et al. Angiogenic and HIV-inhibitory functions of KSHV-encoded chemokines. *Science.* 1997;278(5336):290-294.
19. Aoki Y, Jaffe ES, Chang Y, et al. Angiogenesis and hematopoiesis induced by Kaposi's sarcoma-associated herpesvirus-encoded interleukin-6. *Blood.* 1999;93(12):4034-4043.
20. Sakakibara S, Tosato G. Regulation of angiogenesis in malignancies associated with Epstein-Barr virus and Kaposi's sarcoma-associated herpes virus. *Future Microbiol.* 2009;4(7):903-917.
21. Yao L, Salvucci O, Cardones AR, et al. Selective expression of stromal-derived factor-1 in the capillary vascular endothelium plays a role in Kaposi sarcoma pathogenesis. *Blood.* 2003;102(12): 3900-3905.
22. Samaniego F, Markham PD, Gendelman R, et al. Vascular endothelial growth factor and basic fibroblast growth factor present in Kaposi's sarcoma (KS) are induced by inflammatory cytokines and synergize to promote vascular permeability and KS lesion development. *Am J Pathol.* 1998;152(6):1433-1443.
23. Blankaert D, Simonart T, Van Vooren JP, et al. Constitutive release of metalloproteinase-9 (92-kd type IV collagenase) by Kaposi's sarcoma cells. *J Acquir Immune Defic Syndr Hum Retrovirol.* 1998;18(3):203-209.
24. Bais C, Van Geelen A, Eroles P, et al. Kaposi's sarcoma associated herpesvirus G protein-coupled receptor immortalizes human endothelial cells by activation of the VEGF receptor-2/KDR. *Cancer Cell.* 2003;3(2):131-143.
25. Montaner S, Sodhi A, Servitja JM, et al. The small GTPase Rac1 links the Kaposi sarcoma-associated herpesvirus vGPCR to cytokine secretion and paracrine neoplasia. *Blood.* 2004; 104(9):2903-2911.
26. Wang L, Dittmer DP, Tomlinson CC, Fakhari FD, Damania B. Immortalization of primary endothelial cells by the K1 protein of Kaposi's sarcoma-associated herpesvirus. *Cancer Res.* 2006;66(7): 3658-3666.
27. Wen KW, Damania B. Hsp90 and Hsp40/Erdj3 are required for the expression and anti-apoptotic function of KSHV K1. *Oncogene.* 2010;29(24): 3532-3544.
28. Chandriani S, Ganem D. Array-based transcript profiling and limiting-dilution reverse transcription-PCR analysis identify additional latent genes in Kaposi's sarcoma-associated herpesvirus. *J Virol.* 2010;84(11):5565-5573.
29. Wang L, Damania B. Kaposi's sarcoma-associated herpesvirus confers a survival advantage to endothelial cells. *Cancer Res.* 2008; 68(12):4640-4648.
30. Allingham MJ, van Buul JD, Burridge K. ICAM-1-mediated, Src- and Pyk2-dependent vascular endothelial cadherin tyrosine phosphorylation is required for leukocyte transendothelial migration. *J Immunol.* 2007;179(6):4053-4064.
31. del Pozo MA, Price LS, Alderson NB, Ren XD, Schwartz MA. Adhesion to the extracellular matrix regulates the coupling of the small GTPase Rac to its effector PAK. *EMBO J.* 2000;19(9):2008-2014.
32. Knaus UG, Morris S, Dong HJ, Chernoff J, Bokoch GM. Regulation of human leukocyte p21-activated kinases through G protein–coupled receptors. *Science.* 1995;269(5221):221-223.
33. Vieira J, O'Hearn PM. Use of the red fluorescent protein as a marker of Kaposi's sarcoma-associated herpesvirus lytic gene expression. *Virology.* 2004;325(2):225-240.
34. Sivakumar R, Sharma-Walia N, Raghu H, et al. Kaposi's sarcoma-associated herpesvirus induces sustained levels of vascular endothelial growth factors A and C early during in vitro infection of human microvascular dermal endothelial cells: biological implications. *J Virol.* 2008;82(4): 1759-1776.
35. Servitja JM, Marinissen MJ, Sodhi A, Bustelo XR, Gutkind JS. Rac1 function is required for Src-induced transformation. Evidence of a role for Tiam1 and Vav2 in Rac activation by Src. *J Biol Chem.* 2003;278(36):34339-34346.
36. Manser E, Leung T, Salihuddin H, Zhao ZS, Lim L. A brain serine/threonine protein kinase activated by Cdc42 and Rac1. *Nature.* 1994; 367(6458):40-46.
37. Sells MA, Knaus UG, Bagrodia S, Ambrose DM, Bokoch GM, Chernoff J. Human p21-activated kinase (Pak1) regulates actin organization in mammalian cells. *Curr Biol.* 1997;7(3):202-210.
38. van Wetering S, van Buul JD, Quik S, et al. Reactive oxygen species mediate Rac-induced loss of cell-cell adhesion in primary human endothelial cells. *J Cell Sci.* 2002;115(Pt 9):1837-1846.
39. Braga VM, Machesky LM, Hall A, Hotchin NA. The small GTPases Rho and Rac are required for the establishment of cadherin-dependent cell-cell contacts. *J Cell Biol.* 1997;137(6):1421-1431.
40. Potter MD, Barbero S, Cheresh DA. Tyrosine phosphorylation of VE-cadherin prevents binding of p120- and beta-catenin and maintains the cellular mesenchymal state. *J Biol Chem.* 2005; 280(36):31906-31912.
41. Friedl P, Gilmour D. Collective cell migration in morphogenesis, regeneration and cancer. *Nat Rev Mol Cell Biol.* 2009;10(7):445-457.
42. Wang L, Wakisaka N, Tomlinson CC, et al. The Kaposi's sarcoma-associated herpesvirus (KSHV/HHV-8) K1 protein induces expression of angiogenic and invasion factors. *Cancer Res.* 2004;64(8):2774-2781.

43. An FQ, Folarin HM, Compitello N, et al. Long-term-infected telomerase-immortalized endothelial cells: a model for Kaposi's sarcoma-associated herpesvirus latency in vitro and in vivo. *J Virol.* 2006;80(10):4833-4846.

44. Qian LW, Greene W, Ye F, Gao SJ. Kaposi's sarcoma-associated herpesvirus disrupts adherens junctions and increases endothelial permeability by inducing degradation of VE-cadherin. *J Virol.* 2008;82(23):11902-11912.

45. Mansouri M, Rose PP, Moses AV, Fruh K. Remodeling of endothelial adherens junctions by Kaposi's sarcoma-associated herpesvirus. *J Virol.* 2008;82(19):9615-9628.

46. Dwyer J, Le Guelte A, Galan Moya EM, et al. Remodeling of VE-cadherin junctions by the human herpes virus 8 G-protein coupled receptor. *Oncogene.* 2011;30(2):190-200.

47. Lassègue B, Griendling KK. NADPH oxidases: functions and pathologies in the vasculature. *Arterioscler Thromb Vasc Biol.* 2010;30(4):653-661.

48. Ma Q, Cavallin LE, Yan B, et al. Antitumorigenesis of antioxidants in a transgenic Rac1 model of Kaposi's sarcoma. *Proc Natl Acad Sci U S A.* 2009;106(21):8683-8688.

49. Montaner S, Sodhi A, Molinolo A, et al. Endothelial infection with KSHV genes in vivo reveals that vGPCR initiates Kaposi's sarcomagenesis and can promote the tumorigenic potential of viral latent genes. *Cancer Cell.* 2003;3(1):23-36.

50. Mitsuyasu RT. Update on the pathogenesis and treatment of Kaposi sarcoma. *Curr Opin Oncol.* 2000;12(2):174-180.